Available online at www.sciencedirect.com
SCIENCE DIRECT®
Advances in Space Research 33 (2004) 1763–1770
ADVANCES IN SPACE RESEARCH (a COSPAR publication)
www.elsevier.com/locate/asr

# The ATIC long duration balloon project

T.G. Guzik [a,*], J.H. Adams [b], H.S. Ahn [c], G. Bashindzhagyan [d], J. Chang [e], M. Christl [b], A.R. Fazely [f], O. Ganel [c], D. Granger [a], R. Gunasingha [f], Y.J. Han [g], J.B. Isbert [a], H.J. Kim [g], K.C. Kim [c], S.K. Kim [g], E. Kouznetsov [d], M. Panasyuk [d], A. Panov [d], B. Price [a], G. Samsonov [d], W.K.H. Schmidt [e], E.S. Seo [c], R. Sina [c], N. Sokolskaya [d], M. Stewart [a], A. Voronin [d], J.Z. Wang [c], J.P. Wefel [a], J. Wu [c], V. Zatsepin [d]

[a] Department of Physics and Astronomy, Louisiana State University, 327 C Nicholson Hall, Baton Rouge, LA 70803 4001, USA
[b] NASA Marshall Space Flight Center, Huntsville, AL 35812, USA
[c] Institute for Physical Science and Technology, University of Maryland, College Park, MD 20742, USA
[d] Skobeltsyn Institute of Nuclear Physics, Moscow State University, Moscow 119899, Russia
[e] Max Planck Institut für Aeronomie, Katlinberg – Lindau 37191, Germany
[f] Department of Physics, Southern University, Baton Rouge, LA 70813, USA
[g] Department of Physics, Seoul National University, Seoul 151-742, South Korea

Received 19 October 2002; received in revised form 28 April 2003; accepted 2 May 2003

**Abstract**

Long Duration Balloon (LDB) scientific experiments, launched to circumnavigate the south pole over Antarctica, have particular advantages compared to Shuttle or other Low Earth Orbit (LEO) missions in terms of cost, weight, scientific "duty factor" and work force development. The Advanced Thin Ionization Calorimeter (ATIC) cosmic-ray astrophysics experiment is a good example of a university-based project that takes full advantage of current LDB capability. The ATIC experiment is currently being prepared for its first LDB science flight that will investigate the charge composition and energy spectra of primary cosmic-rays over the energy range from about $10^{10}$ to $10^{14}$ eV. The instrument is built around a fully active, Bismuth–Germanate (BGO) ionization calorimeter to measure the energy deposited by cascades formed by particles interacting in a thick carbon target. A highly segmented silicon matrix, located above the target, provides good incident charge resolution plus rejection of "backscattered" particles from the cascade. Trajectory reconstruction is based on the cascade profile in the BGO calorimeter, plus information from the three pairs of scintillator hodoscope layers in the target section above it. A full evaluation of the experiment was performed during a test flight occurring between 28 December 2000 and 13 January 2001 where ATIC was carried to an altitude of ~37 km above Antarctica by a ~850,000 $m^3$ helium filled balloon for one circumnavigation of the continent. All systems behaved well, the detectors performed as expected, >43 GB of engineering and cosmic-ray event data were returned and these data are now undergoing preliminary data analysis. During the coming 2002–2003 Antarctica summer season, we are preparing for an ATIC science flight with ~15 to 30 days of data collection in the near-space environment of Long Duration Balloon (LDB) float altitudes.


*Keywords:* Scientific ballooning; ATIC long duration balloon project

## 1. Introduction

The ATIC project includes an international collaboration of researchers focused on investigating the spectra of high-energy (>$10^{12}$ eV) galactic cosmic-rays (Guzik et al., 1999). Cosmic-rays are the product of energetic processes in the galaxy, and their interactions with matter and fields are the source of much of the diffuse γ-ray, X-ray, and radio emission that we observe. In addition, these high energy particles are the only sample of matter from distant regions of the galaxy, and possibly elsewhere in the Universe, that can be directly observed

* Corresponding author. Tel.: +1-225-578-8597; fax: +1-225-578-1222.
*E-mail address:* guzik@phunds.phys.lsu.edu (T.G. Guzik).

0273-1177/$30 © 2004 COSPAR. Published by Elsevier Ltd. All rights reserved.
doi:10.1016/j.asr.2003.05.018

by experiments in the solar system. Understanding cosmic-ray origin and acceleration, and how they propagate, is a fundamental problem with a major impact on our understanding of the universe.

Cosmic-ray matter contains all natural elements from hydrogen to beyond nickel. All species have similar energy power law spectra beyond $\sim 10^{10}$ eV/nucleon, where the effects of heliospheric modulation become small. This power law describes the spectra over an enormous energy range, to $>10^{14}$ eV. All-particle measurements (where the species charge cannot be distinguished), principally from ground-based air shower arrays, have traced the spectrum to the highest energies, $\sim 10^{20}$ eV. From these measurements, it has been known for some time that the spectrum is somewhat steeper above $10^{16}$ eV than it is below $10^{14}$ eV. Whether and how this structure, the so-called "knee", is related to the mechanisms of acceleration, propagation, and confinement is one of the major current questions in particle astrophysics.

Fig. 1 shows the summary of high energy data from the National Research Council report "opportunities in Cosmic-Ray Physics and Astrophysics" (Gaisser et al., 1995) as a function of magnetic rigidity for groups of elements. (Here "Fe" refers to $17 \leqslant Z \leqslant 28$.) It was expected that, if all species come from the same sources and have the same propagation history in the galaxy, the spectra at high energy (above $\sim$100 GV in Fig. 1) should have the same shape! This is clearly not the case as inspection of Fig. 1 shows, and several surprising results emerge from the figure. First, the most abundant species, H and He appear to have energy spectra that are different; the flux of He relative to H increasing with energy. Above $\sim$50 TeV, the proton events appear to be less abundant, and this led originally to a report of a possible bend, or break, in the proton spectrum. The heavier nuclei, viewed in charge groups (e.g., C + N + O), show spectra that appear less steep than helium. Extrapolating this trend (naively) to higher energy, the overall composition of cosmic-rays would become dominated by heavy nuclei. However, a range of power law exponents can be encompassed by the dispersion in the heavy nuclei measurements shown, making such extrapolation problematic. The results in Fig. 1 come from a variety of experiments, performed over many years, utilizing various techniques, each covering a limited energy interval. Taken together, the data extend up to $\sim 10^{14}$ eV for protons and to lower kinetic energies for the heavier species. However, the agreement among the experiments is not as good as might be hoped, and the statistical uncertainties at the high-energy end remain large. It is this need for better measurements to understand these spectra that is the experimental rationale for the ATIC investigation.

Concurrently, (over the past 15 years), theorists have developed an attractive and convincing theory of diffu-

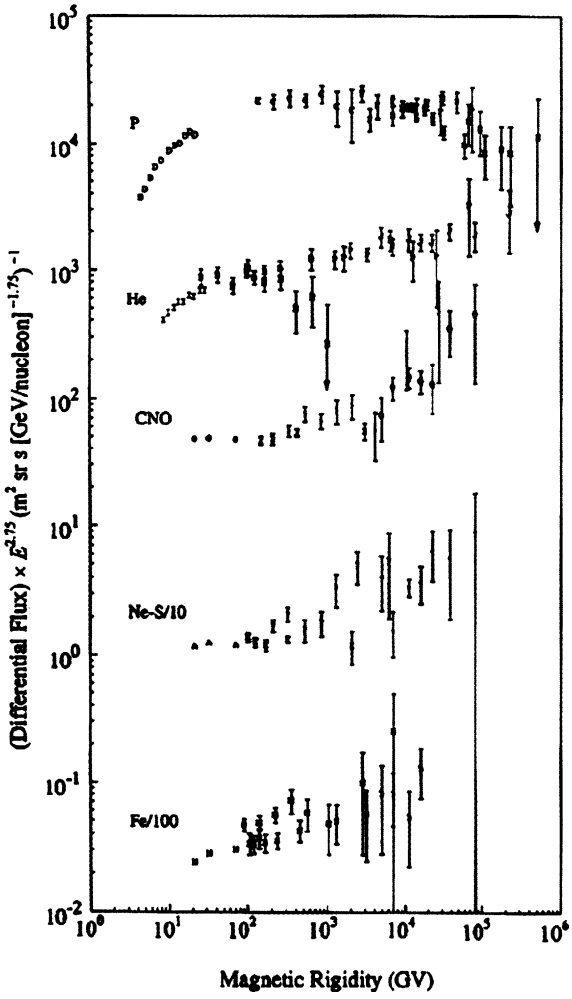


Fig. 1. Compilation of energy spectra for groups of elements.

sive shock acceleration by supernova blast waves that naturally accounts for the essential observed features of most of the relativistic particles in the galaxy. In shock-acceleration, particles pick up a small increment of energy each time they cross the shock boundary in a random-walk (diffusive) process. The maximum energy accessible in a given situation depends on the rate at which the particles diffuse back and forth across the shock and on how long the acceleration mechanism acts. For a supernova (SN) shock, the available acceleration time is limited by the time taken for the blast wave to propagate outward into the ISM and to weaken to the point that it is no longer an efficient accelerator. In the most commonly used form of the theory, the characteristic, "limiting" energy is $E = Z \times 10^{14}$ eV, where $Z$ is the particle charge (e.g., Lagage and Cesarsky, 1983). This implies that the composition would begin to change in the energy region around $10^{14}$ eV, since this is the limiting energy for protons. However, changing the assumed magnetic field topology or field strength or the characteristics of the medium into which the SNR is

expanding (Ellison et al., 1994) results in changing the predicted maximum energy for the accelerated particles.

Fig. 2 shows updated spectra for H and He, with the flux again multiplied by $E^{2.75}$ including recent results from the Japanese American Cooperative Emulsion Experiment (JACEE, Asakimori et al., 1998, filled circles H, open circles He) and the Russian–Nippon Joint Balloon program (RUNJOB, Shibata, 1996; Apanasenko et al., 2001 open circles H, filled triangles He). Comparison to Fig. 1 shows that the apparent fall off at the highest energies for protons is no longer prominent, due, mainly, to refined data from the JACEE group, who report spectra consistent with single power laws. However, Cherry et al. (1999), using a maximum likelihood analysis, show that a spectral break above ~40 TeV cannot be ruled out. The statistical significance of the data is just not high enough to draw a conclusion one way or the other. Other analyses (e.g., Zatsepin and Sokolskaya, 1999; Grigorov and Tolstaya, 1999) still favor a spectral break, so this remains an unanswered question.

The spectral fits shown in Fig. 2 still favor a difference in the spectral index for hydrogen and helium at the two sigma level with an index change of $0.12 \pm 0.06$. A difference in the spectral indices would almost certainly signify two different types of sources or acceleration mechanisms for H and He (e.g., Biermann, 1993; Zatsepin, 1995). However, RUNJOB recently reported H and He spectra that show the same index (Apanasenko et al., 2001). What is needed to understand the spectral shapes is a set of measurements covering the full energy range with a single instrument of demonstrated capability, a major goal of the ATIC investigation.

In summary, the objectives for ATIC are: (1) Measure the H and He energy spectrum from $\sim 10^{10}$ to $\sim 10^{14}$ eV with a single instrument. (2) Confirm or refute the spectral differences between protons and helium. (3) Determine if the proton spectrum shows any feature above ~1 TeV. (4) Accurately measure the H/He ratio as a function of energy. (5) Determine if the spectra of heavy nuclei have the same indices.

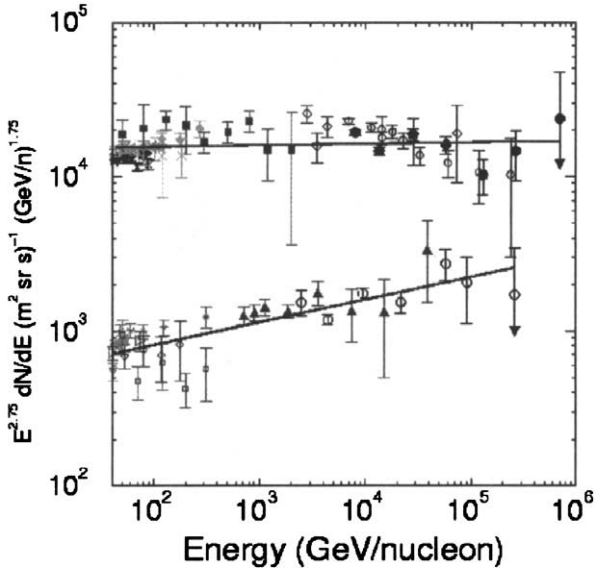


Fig. 2. Compilation of measurement for H (top) and He (bottom).

## 2. The ATIC experiment payload

The only practical method of energy determination over a broad energy range for $Z \geqslant 1$ particles seems to be ionization calorimetry. In an ionization calorimeter a particle's energy is deposited via a cascade of nuclear and electromagnetic interactions. Fig. 3 shows a schematic of the ATIC experiment with a simulation of a high energy proton interacting and generating such a cascade. At each step of the cascade, the energy of the parent particle is sub-divided among many daughter particles. The area under the curve of ionization energy versus depth in the medium provides a measure of the particle energy. In principal, an infinitely deep calorimeter provides energy resolution limited only by the statistical nature of the cascade process and the measuring technique. Practical calorimeters for balloon applications must necessarily be limited in thickness to have a reasonable cross sectional area, i.e., geometrical factor, and a "flyable" weight. In such detectors the resolution is limited by fluctuations in the energy fraction carried by electromagnetically interacting particles (e.g., $\pi^0$ mesons, and mostly those formed in the first interaction).

For ATIC, we have developed an advanced calorimeter based upon fully active Bismuth–Germanate (BGO) scintillating crystals (1.12 cm per radiation length or $X_0$) following a 30 cm carbon target (25 cm per $X_0$). The incident particle interacts in the carbon, but the majority of the shower develops in the BGO. For our LDB flights from McMurdo, the calorimeter, shown in Fig. 4, consists of eight layers of 2.5 cm thick BGO crystals giving a vertical calorimeter depth of 17.9 $X_0$. A layer includes 40 BGO crystals of dimensions 2.5

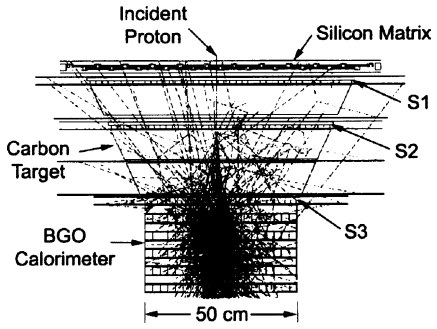


Fig. 3. An example of a simulated proton shower in the McMurdo flight configuration.

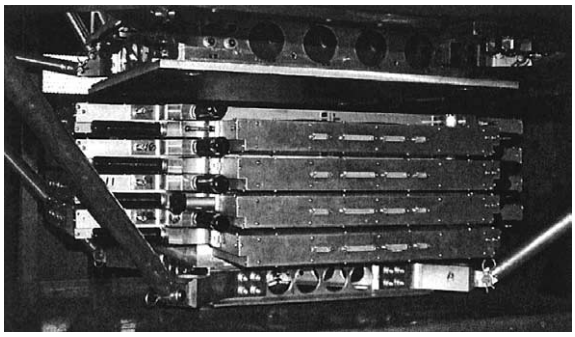

Fig. 4. ATIC BGO calorimeter trays.

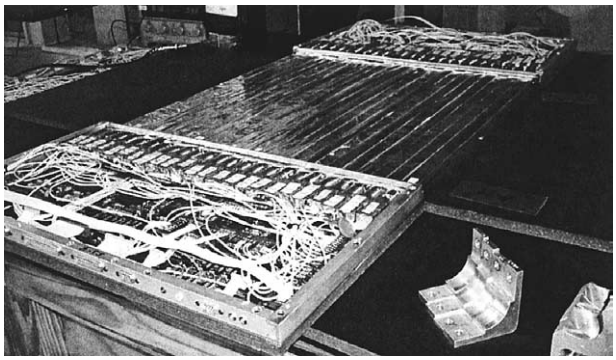

Fig. 6. One of two S3 hodoscope layers.

cm × 2.5 cm × 25 cm, with each crystal viewed by a Hamamatsu R5611 photomultiplier tube.

The instrument must also determine the charge of the incident particle and measure its trajectory through the apparatus. At the top of the instrument (Fig. 3) is a silicon detector to determine the charge of the incident particle. In a calorimeter, there is always some "backsplash" of particles emitted or scattered into the backward hemisphere that can confuse the charge measurement. To resolve this problem, the Silicon Matrix (Fig. 5), which includes 4480, 2 cm × 1.5 cm "pixels" mounted on offset ladders, allows separation of the backscatter noise from the incident particle signal. The total active area of the Silicon Matrix is 0.95 m × 1.05 m. In addition, crossed plastic scintillator strip hodoscope layers are located at the top, bottom and within the carbon target (S1, S2 and S3 in Fig. 3) to provide triggering (geometry definition) and auxiliary charge information as well as tracking information to be combined with the location of the shower core from the calorimeter. Each hodoscope is of similar construction (Fig. 6) though the length and number of strips varies with the position of the layer in the instrument. For S1, 84 strips of Bicron BC-408 of dimensions 2 cm × 1 cm × 88.2 cm are used, while S2 includes 70 strips 74.2 cm long and S3 has 48 strips that are 52.4 cm long. As seen in Fig. 6, each strip has a Hamamatsu R5611 on each end to provide redundant readout capability. Finally, 16 channel, 16 bit CR-1 application-specific integrated circuits (ASIC) (Adams et al., 1999) are used for the Silicon Matrix readout, while ASICs based on the design used for the ACE mission, including 16 input channels, two "trigger" output signals as well as 12 bit digitized pulse heights are used for the BGO and hodoscope readout.

ATIC has been designed specifically as a LDB payload, meeting stringent weight requirements and launch conditions. The total weight of ATIC is about 3400 lb and the structure is capable of withstanding the loads associated with launch, parachute deployment and landing. Further, the instrument is highly modular providing for easy break down in the field and allowing the resulting components to be loaded onto a variety of recovery platforms. Once tuned for flight, ATIC generates an average of ~275 kbps of data that can be downlinked during the first 10 to 20 h of flight while the payload is in line-of-sight (LOS). Once out of LOS, telemetry is limited to the 4–6 kbps TDRSS bandwidth. Thus, ATIC includes a ~70 GB disk for on-board data recording, a priority queue for preferentially transmitting important housekeeping/monitoring data and failure detection/recovery software for semi-autonomous operations. The payload is contained in a Kevlar pressure vessel that maintains a ~8 psi environment for the instrument. It utilizes photovoltaic arrays to supply the 250 W of science power needed during flight (an additional 160 W was allocated for thermal control heaters, but these heaters were not needed during flight).

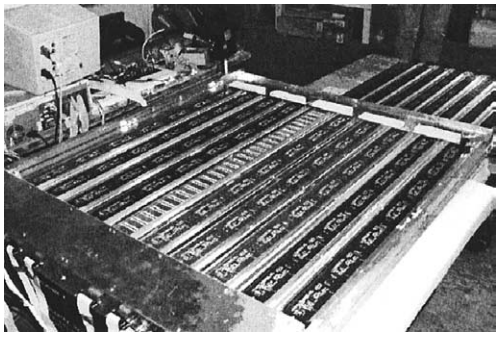

Fig. 5. ATIC Silicon Matrix detector.

## 3. The ATIC test flight

All LDB payloads are required to perform a short "test" flight to assure system performance and our group was anticipating this flight for Fall, 2000 at Ft. Sumner, New Mexico and then the Antarctica LDB flight the following year. Circumstances, however, allowed NASA to invite ATIC to move its schedule forward and perform the "test" flight from McMurdo, Antarctica during the 2000–2001 season. After several months of intense preparation (at Louisiana State Uni-

versity (LSU), the National Scientific Balloon Facility (NSBF) in Palestine, TX, and on the flight line in Williams Field, Antarctica) ATIC was launched for the first time on 12/28/2000 at 04:25 UTC. The rollout of the payload from the integration hangar at Williams Field to the launch pad is shown in Fig. 7.

The launch went smoothly, the payload reached altitude within a couple of hours and remained within LOS for almost 24 h. During this LOS period we were able to check instrument performance and set the trigger thresholds. Nominal data collection began once the payload left LOS on 12/29/00 at 03:54 UTC and continued for the next ~350 h as the experiment circumnavigated the Antarctic continent. The ATIC balloon path, as recorded by the NSBF, is shown in Fig. 8.

During the ATIC flight, the payload altitude was $37 \pm 1.5$ km, the instrument temperature stayed in the range 20–30 °C and the internal pressure remained at ~8 psi with no detectable leakage. Over the course of the flight ATIC recorded over 43 GB of data including 26,100,000 cosmic-ray triggers, 1,300,000 calibration records, 742,000 housekeeping records, 18,300 rate records, all with >90% of detector channels operating nominally. The instrument was powered off on 1/12/01 at 20:33 UTC in preparation for flight termination which occurred 1/13/01 at 03:56 UTC. The payload landed upright, largely intact and was essentially fully recovered during two Twin Otter flights to the landing site on 1/23/01 and 1/25/01.

In general the payload worked well during the test flight. ATIC operated for more than 14 days with little ground intervention, collecting data on high energy cosmic-ray events. We were able to monitor instrument health and performance during the full flight via TDRSS and LOS telemetry, and to modify experiment settings when necessary with uplinked commands. Throughout the flight, the Kevlar pressure vessel worked flawlessly.

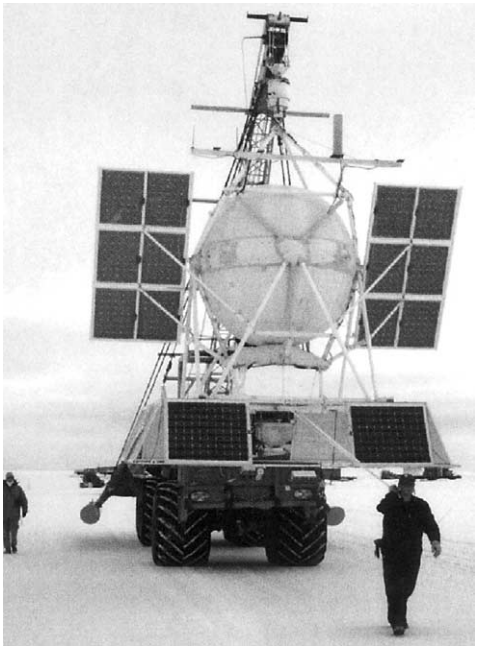

Fig. 7. Roll out of ATIC to launch on 12/28/00.

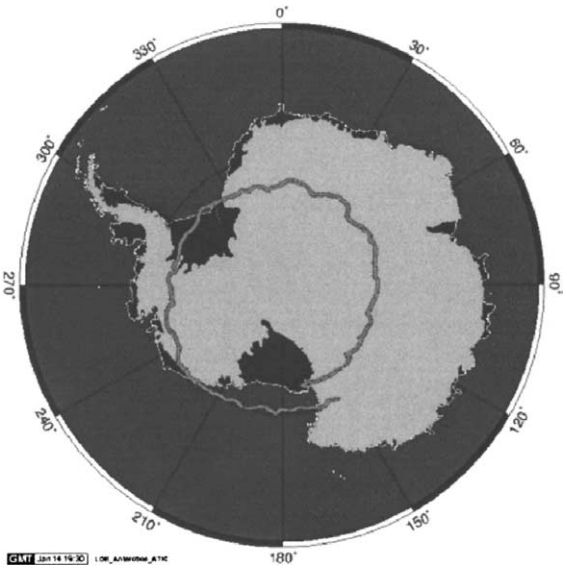


Fig. 8. Path of ATIC during 2000–2001 flight.

However, we did have our share of problems during the flight. For example: a few data files were corrupted during flight; some command records in the flight data were invalid and we had a problem with receiving command acknowledgements; a software defect allowed the GPS clock to occasionally hang the Detector Control Unit (DCU) computer stack, causing us to remove the GPS clock for the 2000 flight; only two of the rate counters appear to be valid; the PMTs on one side of one layer of S2 failed to function shortly before launch and on one side of one layer of S1 two days into the flight resulting in the loss of the redundant readout for these two layers. Since the recovered ATIC components were returned to the US in April 2001, LSU has spent most of 2001 and 2002 understanding and fixing the issues found during the test flight, modifying the payload to incorporate "lessons learned" to enhance performance/recoverability, and refurbishing ATIC to prepare for its science flight during the 2002–2003 Antarctica season.

Analysis of the ATIC "test" flight data has been used to examine the performance of the instrument and to obtain some preliminary results. One critical parameter to be examined is the energy dependence of the trigger, so that any such effects can be removed from the measured cosmic-ray flux energy spectrum. Figs. 9 and 10 show some preliminary results on the ATIC trigger. Fig. 9 shows the Gated Master Trigger (MT) count rate versus mission days. The initial data collection period has a count rate of about 2000 and lasts from about the

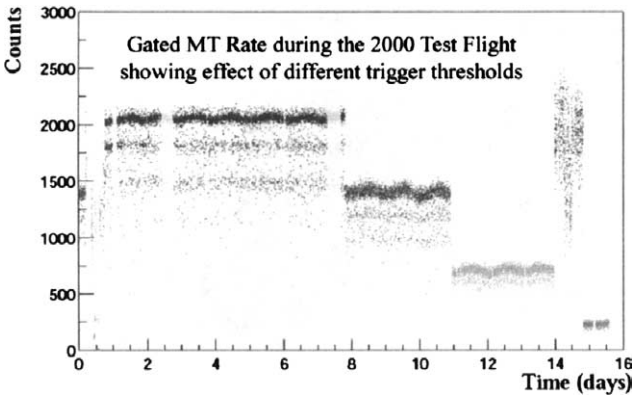


Fig. 9. The MT count rate.

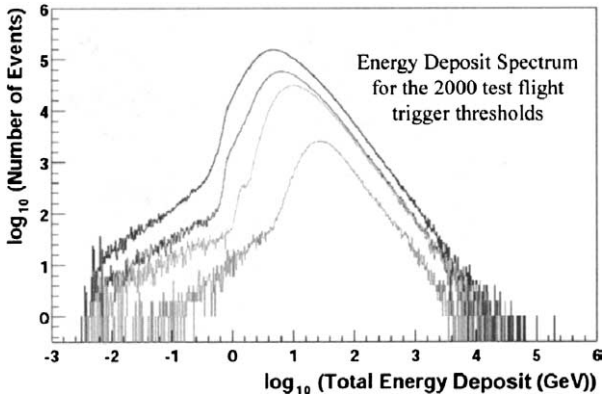


Fig. 10. The energy deposit spectrum.

time of LOS loss to about day 7. The lighter bands at a count rate of about 1800 and 1500 are due to dead time effects. The cyclic variation in the count rate has a time period a little more than a day and is likely due to the "daily" variation in the balloon altitude. Over the course of the mission we increased the trigger thresholds on the BGO calorimeter signals three times. These increases correspond to the decreased Gated MT count between days ~8–11 (MT ~1500), days 11–14 (MT ~750) and day 15 (MT ~250). During day 14 a different trigger configuration was used to collect some detector performance data. In Fig. 10, the all particle energy deposit (in the calorimeter) spectrum corresponding to each of the four trigger thresholds can be seen. The top curve was determined from data taken during period 1 (i.e., days 1–7), the next lower curve during period 2 (i.e., days 8–11), and so on. From Fig. 10 we see that the effect of the energy dependence in the trigger varies according to the threshold setting, but by about 100 GeV total energy deposit the trigger appears to be close to 100% efficient. In fact, between ~100 GeV and ~5 TeV total energy deposit very reasonable power law spectra are apparent. However, much beyond ~5 TeV total energy deposit, low statistics become a problem.

Another critical measurement made during the test flight was the charge resolution capability of the Silicon Matrix detector in the presence of shower "backscatter". Fig. 11 shows the charge histogram for Li–Ne using the "hit" pixels in a single Silicon Matrix layer. The "hit" pixel was determined by back tracing the particle trajectory determined from the shower core in the BGO calorimeter. In this case, primary elements such as C and O as well as H and He (not shown) are well resolved, but the lower abundant secondary species (i.e., Be, B, N, F) are not all clearly resolved. Due to the multi-layer construction of the Matrix, a portion of the particle trajectories (~15%) will actually pass through two silicon pixels on two different layers. By requiring charge consistency in both pixels, a more accurate measurement of the incident particle charge can be obtained. The resulting "Double Layer" charge histogram for the Li–Ne region is given as Fig. 12, which shows that all elements are now well resolved. Similar improvement in charge resolution was found for H and He as well for elements Ne through Fe. Charge calibrations for the S1 hodoscope layer, located directly under the Silicon Matrix,

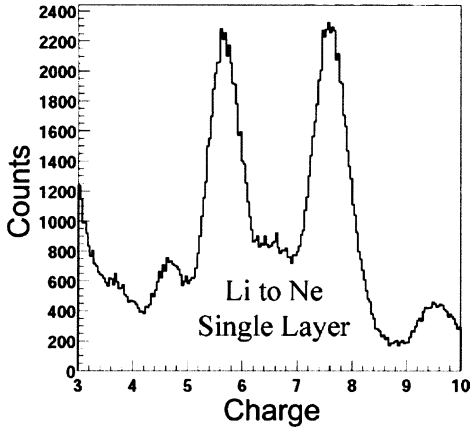


Fig. 11. Silicon Matrix single layer charge histogram for Li to Ne.

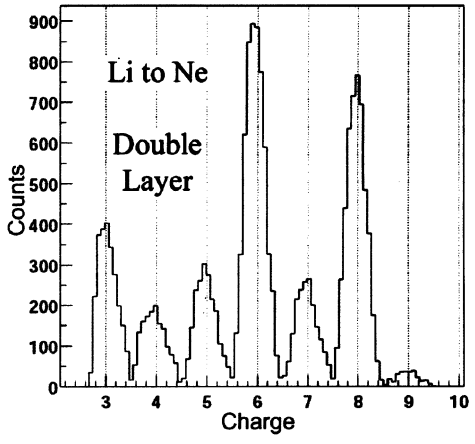


Fig. 12. Silicon Matrix double layer charge histogram for Li to Ne.

are still underway, but once they are complete we will be able to use S1 for charge consistency checks for all particles passing through the Matrix significantly increasing the charge resolution beyond that shown in Fig. 11.

Finally, Fig. 13 shows the charge resolution for H and He using a single Silicon Matrix layer and Fig. 14 shows the He/H elemental ratio and CNO/He ratio versus rigidity obtained from the ATIC test flight data. For both elemental ratios the rigidity dependence seen for rigidity less than ~50 GV may be due to the energy dependence in the trigger threshold (i.e., see Fig. 10). Also in both cases the ratio is more or less constant between 100 GV and ~1 TV. The data is also consistent with a constant ratio for energies >1 TV, but beyond 3–4 TV the low statistics do not allow hard conclusions to be drawn. Further time aloft by the ATIC instrument will allow more data to be gathered at these highest energies.

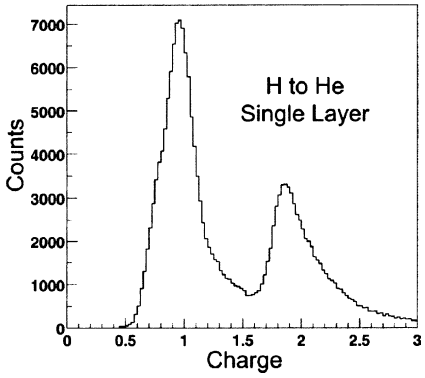


Fig. 13. Silicon Matrix charge histogram for H and He.

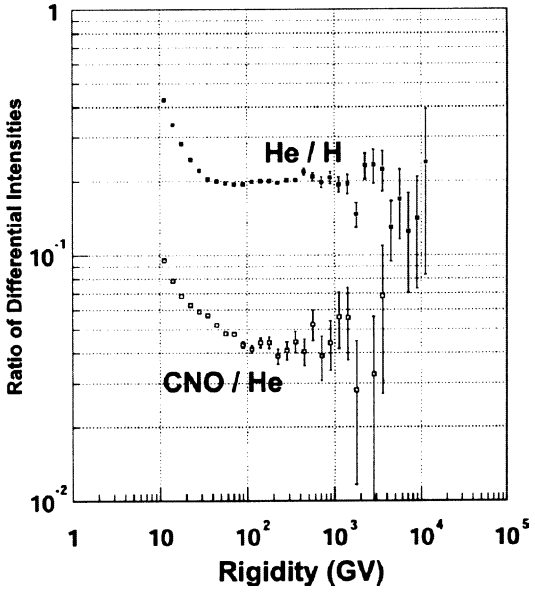


Fig. 14. Preliminary CNO/He ratio.

## 4. Conclusions

The ATIC experiment is designed to study the charge composition and energy spectra of primary cosmic-rays over the energy range from about $10^{10}$ to $10^{14}$ eV. The instrument uses a BGO ionization calorimeter to determine incident particle energy and trajectory through the detector stack, a highly segmented silicon matrix detector to determine cosmic-ray charge and plastic scintillator hodoscopes to provide the instrument trigger as well as supplementary information on particle charge and trajectory. In addition, the payload has been designed to take into account the weight, recovery and operational constraints associated with LDB flights. On 12/28/2000 ATIC was launched from Williams Field in Antarctica for a ~15 day test LDB flight. The experiment performed well during this test, but some problems were encountered. Nevertheless, the recovered data provided important information on the trigger energy dependence, charge resolution and other performance measures. In addition, preliminary He/H and CNO/He ratios appear to be energy independent over the range 100 GV to ~1 TV magnetic rigidity. During 2001 and 2002 the recovered components of ATIC were refurbished, modified to incorporate lessons learned during the test flight and assembled in preparation for the 2002 science flight. Pre-deployment integration occurred at NSBF in Palestine, TX during July, 2002, and the instrument was shipped to Antarctica. Currently, ATIC is being prepared for flight at Williams Field and is expected to be flight ready by 12/15/2002. If conditions permit we will attempt to circumnavigate the Antarctic continent twice this season providing ~30 days of science data. [Note added in proof: The ATIC payload was launched from Williams Field 29 December 2002 at 4:59 UTC and was terminated 18 January 2003 at 2:01 UTC resulting in a very successful 19 day mission at float collecting data on ~16.9 million cosmic-ray events. Preliminary analysis of these data is now underway. The payload was recovered, returned to LSU and is now awaiting refurbishment.]

## Acknowledgements

The ATIC effort is supported at Louisiana State University – Baton Rouge by NASA Grant Nos. NAG5-5064 and NAG5-5306 and the Louisiana Board of Regents; at University of Maryland by NASA Grant No. NAG5-5155; at Southern University – Baton Rouge and Marshall Space Flight Center by NASA; at Moscow State University by the Russian Foundation for Basic Research Grant Nos. 02-99-16246 and 02-02-16545. We are also grateful for the support and professionalism of the NASA National Scientific Balloon Facility personnel as well as to the NSF Office of Polar

Programs and Raytheon Polar Services Company (RPSC) for their logistical support during the ATIC 2000–2001 and 2002–2003 Antarctica campaigns.

## References

Adams Jr., J., Ampe, J., Bashindzhagyan, G., et al. The CR-1 chip: custom VLSI circuitry for cosmic rays, in: Proceedings of the 26th International Cosmic Ray Conference, Salt Lake City, vol. 5, pp. 69–71, 1999.

Apanasenko, A.V., Beresovskaya, V.A., Fuji, M., et al. Proton and helium spectra observed by RUNJOB, in: Proceedings of the 27th International Cosmic Ray Conference, Copernicus Gesellschaft, Katlenburg–Lindau, vol. 5, pp. 1626–1629, 2001.

Asakimori, K., Burnett, T.M., Cherry, M.L., et al. Cosmic ray proton and helium spectra – Results from the JACEE experiment. Ap. J. 502, 278–283, 1998.

Biermann, P.L. Cosmic rays: origin and acceleration, what we can learn from radioastronomy, in: Leahy, D.A., Hicks, R.B., Venkatesan, D. (Eds.), Proceedings of the 23rd International Cosmic Ray Conference Calgary. World Scientific, Singapore, pp. 45–83, 1993.

Cherry, M.L., Asakimori, K., Burnett, T.M., et al. Where is the bend in the cosmic ray proton spectrum? in: Proceedings of the 26th International Cosmic Ray Conference, Salt Lake City, vol. 3, pp. 187–190, 1999.

Ellison, D.C., Reynolds, S.P., Borkowski, K., et al. Supernova remnants and the physics of strong shock waves. Publ. Astron. Soc. Pacific 106, 780–797, 1994.

Gaisser, T.K., Caldwell, D.O., Cronin, J., et al. Opportunities in Cosmic-Ray Physics and Astrophysics. National Research Council, National Academy Press, Washington, DC, 1995.

Grigorov, N.L., Tolstaya, E.D. The process leading to the formation of a 'Knee' in the proton spectrum at energies of about 1 TeV, in: Proceedings of the 26th International Cosmic Ray Conference, Salt Lake City, vol. 4, pp. 464–466, 1999.

Guzik, T.G., Adams Jr., J., Ampe, J., et al. The advanced thin lonization calorimeter (ATIC) for studies of high energy cosmic rays, in: Proceedings of the 26th International Cosmic Ray Conference, Salt Lake City, vol. 5, pp. 9–12, 1999.

Lagage, P.O., Cesarsky, C.J. The maximum energy of cosmic rays accelerated by supernova shocks. Astron. Astrophys. 125, 249–257, 1983.

Shibata, T. Cosmic ray spectrum and composition: direct observation. Nuovo Cimento C 19, 713–736, 1996.

Zatsepin, V.I. Primary proton spectrum above 1 TeV and the problem of cosmic-ray origin. J. Phys. G. 21, L31–L34, 1995.

Zatsepin, V.I., Sokolskaya, N.V. Two components in the galactic cosmic rays, in: Proceedings of the 26th International Cosmic Ray Conference, Salt Lake City, vol. 4, pp. 136–139, 1999.